JOURNAL OF CATALYSIS 118, 443–458 (1989)

The Genesis of Carbon-Supported Fe–Mn and K–Fe–Mn Catalysts from Stoichiometric Mixed-Metal Carbonyl Clusters

II. Characterization by Mössbauer Spectroscopy and TEM/EDS

A. A. CHEN, J. PHILLIPS, J. J. VENTER, AND M. A. VANNICE[1]

Department of Chemical Engineering, The Pennsylvania State University, University Park, Pennsylvania 16802

Received September 13, 1988; revised April 12, 1989

Mössbauer effect spectroscopy (MES) and transmission electron microscopy/energy-dispersive X-ray spectroscopy (TEM/EDS) were used to study the chemistry of the iron particles produced by the thermal decomposition of stoichiometric K–Fe, Fe–Mn, and K–Fe–Mn mixed-metal carbonyl clusters on a high surface area carbon. Intermediate chemical states during the cluster decomposition process below 473 K were identified using MES, and they indicated that decarbonylation occurred via the formation of $Fe(CO)_5$ and $[Fe_4(CO)_{13}]$ during heating in H_2. Following decomposition at 473 K, the principal final phase was the D-structure, which has been associated with superparamagnetic Fe combined with an Fe^{2+} state. Additionally, a doublet characteristic of Fe^{3+} oxide and/or superparamagnetic carbide appeared in the spectrum. No evidence for a mixed spinel such as Fe_2MnO_4 was obtained, but the Fe and Mn appeared to remain in contact, presumably as MnO_x on top of small Fe crystallites. A subsequent treatment in H_2 at 673 K caused the K-promoted catalysts to sinter and form separate phases of Mn oxide and large particles of α-Fe, as detected by MES and TEM/EDS. For the unpromoted Fe–Mn sample, little sintering occurred under H_2 at 673 K, and the particles existed in a phase which has been previously found in Fe-only carbon-supported catalysts.

INTRODUCTION

Numerous investigations have recently been conducted on reduced Fe–Mn oxides, largely because of their potential to selectively produce olefins via CO hydrogenation. The catalytic properties of bulk Fe–Mn catalysts in this reaction are well documented in both the patent and the research literature (*1–15*), but only a few studies have been directed at elucidating the properties of small, supported Fe–Mn particles (*16–18*). Within this latter class of catalysts, it has been shown that carbon-supported particles derived from stoichiometric Fe–Mn and K–Fe–Mn carbonyl clusters have excellent selectivity to C_2–C_4 olefins and high activity in the CO hydrogenation reaction (*18*). In particular, it was found that $N(C_2H_5)_4[Fe_2Mn(CO)_{12}]$ clusters produced catalysts which were highly selective to light olefins after a pretreatment in H_2 at only 473 K, and it was proposed that this selectivity was due to the existence of an $(Fe_{1-y}Mn_y)_3O_4$ spinel phase (*18*) because of the association of high olefin selectivity with the spinel structure in bulk catalyst systems (*12–15*).

Whereas the phase behavior of these large Fe–Mn particles has been intensively investigated (*1–15*), little is known about the metal phases that are present in very small Fe–Mn particles. The use of stoichiometric mixed-metal carbonyl clusters not only produces small promoted Fe particles, but also provides a single initial species with zero-valent iron which facilitates characterization. The use of a clean, oxygen-free carbon support with high surface area provides additional benefits because it does not produce the metal oxidation observed on oxide supports (*19*), and it gives stable,

[1] To whom correspondence should be addressed.

0021-9517/89 $3.00

well-dispersed, zero-valent iron phases with a reproducible unique structure when Fe-only clusters are used. However, the capability of carbon to achieve this with manganese or potassium present on its surface has not been determined. Thus the combination of these mixed-metal clusters with carbon represents a unique system that had not yet been characterized.

The decomposition of these clusters on carbon has now been studied by DRIFTS (diffuse reflectance fourier transform infrared spectroscopy) and these results are discussed in the first paper of this series (*20*). The third paper presents CO heat of adsorption measurements, illustrates the kinetic behavior of these catalysts for CO hydrogenation, proposes a model describing the decomposition pathway for these clusters, and relates catalytic behavior to the final state of the catalyst (*21*). The present paper provides the first Mössbauer investigation of these supported mixed-metal clusters and the iron phases produced on carbon after their decomposition. It also provides a study of the influence of potassium on the behavior of the iron/carbon system. The Mössbauer effect spectroscopy (MES) data reported here are shown to be consistent with the DRIFTS decarbonylation results up to 473 K and, in addition, the structure of the particles was determined following pretreatment at 673 K in H_2. Even though the Fe and Mn are initially bonded to each other in the cluster precursors, they do not appear to form a homogeneous Fe–Mn bulk phase following cluster decarbonylation. After pretreatment at 673 K, potassium-promoted Fe and Fe–Mn catalysts form large Fe particles, while an unpromoted Fe–Mn catalyst remains well dispersed.

EXPERIMENTAL PROCEDURE

The metal carbonyl precursors $NEt_4[Fe_2Mn(CO)_{12}]$ (*22*), $K[Fe_2Mn(CO)_{12}]$ (*22*), $K[FeMn(CO)_9]$ (*22*), and $K[HFe_3(CO)_{11}]$ (*23*), where Et represents the ethyl radical, were prepared according to previously published techniques. The carbon support used, Cabot CSX-203, is now commercially available from Cabot Corp. as "Black Pearls 2000." The carbon was heated at 1123 K under a flow of H_2 for 12 h, after which it was cooled to room temperature under flowing H_2. The carbon was then transferred without air exposure to a nitrogen-purged glovebox for storage. All impregnations were performed using standard Schlenk techniques under a N_2 atmosphere (*24*). Using dried, degassed THF as the solvent, the carbon was impregnated to give catalysts with approximately 10 wt% total metal loading which were subsequently evacuated for 8 h at 0.13 Pa to remove the excess THF. The dried catalysts were transferred to the MES cell under a N_2 atmosphere.

The MES spectra were collected using two different cells, hereafter referred to as the HT (high temperature) cell and the LT (low temperature) cell. The HT cell allows *in situ* sample treatments and spectrum collection in any gas or vacuum (0.13 Pa) over a temperature range of 77 to 723 K. This cell has been described in more detail elsewhere (*25*). Spectra at 10 K were obtained using the LT cell, an Air Products Liquid Transfer Helitran, Model LT-3-110, which can operate in the temperature range of 4 to 298 K. Prior to obtaining the 10 K spectra, the samples were pretreated in the HT cell and transferred to the LT cell inside the N_2-purged glovebox. All spectra were obtained in the constant acceleration mode and all isomer shifts are reported with respect to α-Fe at room temperature. The H_2 (Linde, 99.999%) and CO (Matheson, 99.99%) were further purified by passing them through an Oxytrap (Alltech Associates) and a molecular sieve trap before use.

The spectra were fitted by the program MFIT (*26*). This program fits the data to an assigned number of Lorentzian lines superimposed on a horizontal baseline. The fitting is "least squares" employing a random stepping of free parameters to find the best fit. For the unrelaxed spectra, the sextuplets were constrained such that (i) the separations between lines were consistent with

the known nuclear magnetic moment of Fe, and (ii) the dips and widths of the peaks at negative velocity were equal to those of corresponding peaks at positive velocity. The peaks comprising quadrupole doublets were constrained to have equal dips and widths. The free parameters were the quadrupole splitting and the hyperfine fields. The fitting of both carbide and partially relaxed spectra was performed only to derive an approximate hyperfine splitting for the phases present.

Air-exposed catalyst samples were prepared for electron microscopy by stirring them in acetone and then placing the mixture in an ultrasonic bath for 5 min. The resulting suspension was placed dropwise on 400-mesh Cu grids which had been precoated with a carbon film. The grids were dried briefly using a heat lamp prior to insertion into the microscope. The samples were imaged on a Philips 420 STEM operating in the TEM mode at 120 keV, and all EDS data were collected using a Link Systems EDS attached to the STEM. For EDS analyses, the electron beam was focused to a spot size of 30–70 nm and placed on the desired area while the microscope stage and grid were tilted at 20–35° relative to horizontal. The relative amounts of K, Fe, and Mn were estimated using the peak intensities and previously published Cliff–Lorimer factors referenced to Fe at 120 keV (*27*).

RESULTS

To investigate the decomposition behavior of the supported clusters, the samples were pretreated in H_2 using the HT MES cell. First, a MES spectrum of the freshly impregnated sample was taken at 77 K. Following this, the clusters were decarbonylated by heating to 323, 373, 423, and 473 K in an atmosphere of H_2. The cell was held at each of the first three temperatures for 1 h and after each temperature it was cooled to 298 K in flowing H_2, evacuated, and cooled to 77 K for spectrum collection. The results obtained are presented sequentially below.

1. Fresh Catalysts

Figure 1 shows the MES spectra obtained on the fresh $NEt_4[Fe_2Mn(CO)_{12}]$, $K[FeMn(CO)_9]$, and $K[HFe_3(CO)_{11}]$ catalysts after impregnation and evacuation to remove THF, and the MES parameters are given in Table 1. The $K[Fe_2Mn(CO)_{12}]$ sample gave a spectrum (not shown) nearly identical to the $NEt_4[Fe_2Mn(CO)_{12}]$ sample (Fig. 1a), consistent with the fact that both of the catalyst precursors contained the same $[Fe_2Mn(CO)_{12}]^-$ anion. Spectra 1a and 1b agree well with those published for unsupported $NEt_4[Fe_2Mn(CO)_{12}]$ (*28, 29*) and $[HFe_3(CO)_{11}]^-$ clusters (*30*), respectively, indicating that all of the clusters remained intact on the carbon surface. The $K[FeMn(CO)_9]$ sample gave a spectrum (Fig. 1c) consisting of two doublets whose parameters matched those of $[Fe_2Mn(CO)_{12}]^-$ anions and $Fe(CO)_5$. MES parameters for the unsupported cluster are also given in Table 1 for comparison.

Attempts were made to image the freshly impregnated $NEt_4[Fe_2Mn(CO)_{12}]$ catalyst in the TEM; however, no distinct metal particles were observed, a result which might be expected if the carbonyl clusters were dispersed in molecular form. Despite this, Fe and Mn were detected by EDS throughout the sample. Semiquantitative analyses of seven different areas yielded Fe : Mn ratios of 2 : 0.80 to 2 : 1.16, in approximate agreement with the stoichiometric ratio found in the cluster precursor. The appearance of the $K[Fe_2Mn(CO)_{12}]$ sample was similar to the $NEt_4[Fe_2Mn(CO)_{12}]$ catalyst in that no individual metal particles could be imaged. Again, the Fe : Mn ratios were in agreement with that expected from the cluster precursor, although the peak for K was too weak to be seen. During the analysis of a larger (830 nm diam) area in this catalyst, K was detected, but the final composition was $K_{0.56}Fe_2Mn_{0.95}$. The absence of any large particles of metal in these catalysts is consistent with earlier reports of high initial dispersions for these cluster-derived catalysts (*18*).

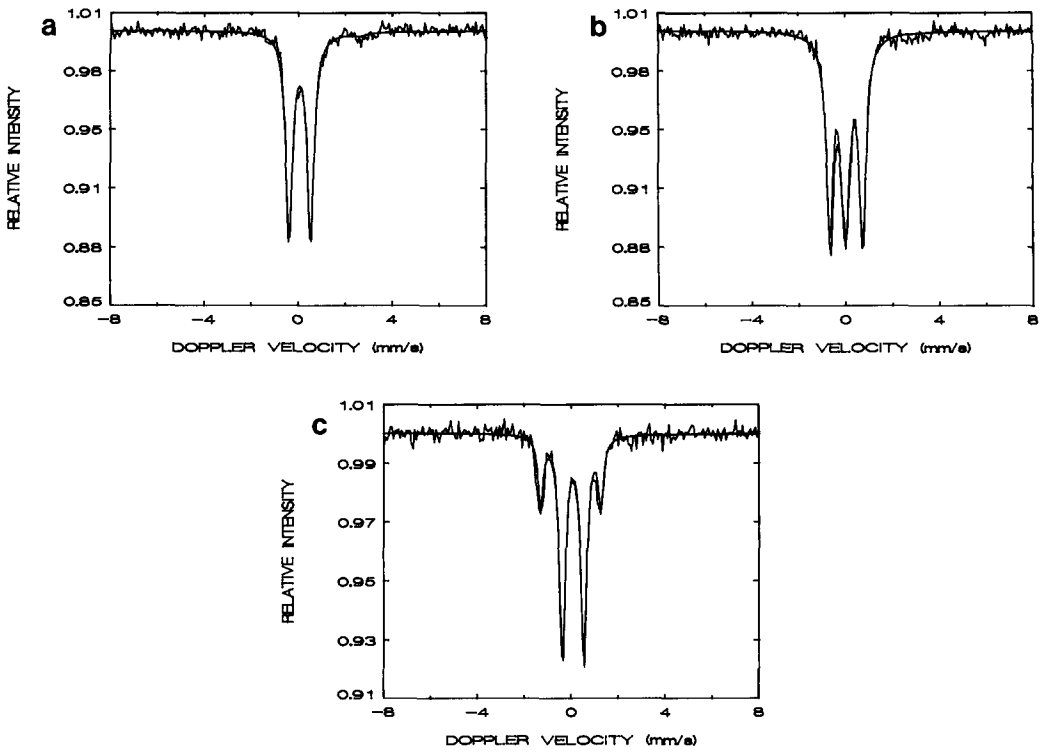

FIG. 1. Mössbauer spectra at 77 K of freshly impregnated catalysts following 8 h evacuation to remove THF: (a) $NEt_4[Fe_2Mn(CO)_{12}]$ catalyst, (b) $K[HFe_3(CO)_{11}]$ catalyst, and (c) $K[FeMn(CO)_9]$ catalyst.

II. Cluster Decarbonylation

The spectra obtained after heating at 323 K for 1 h are shown in Fig. 2. The sample prepared from $NEt_4[Fe_2Mn(CO)_{12}]$ contained two additional species. One produced the small peak to the left of the central doublet that is paired with a partially hidden peak to the right, causing a slight broadening at approximately 1.2 mm/s. The isomer shift and quadrupole splitting are indicative of $Fe(CO)_5$, which was also seen in

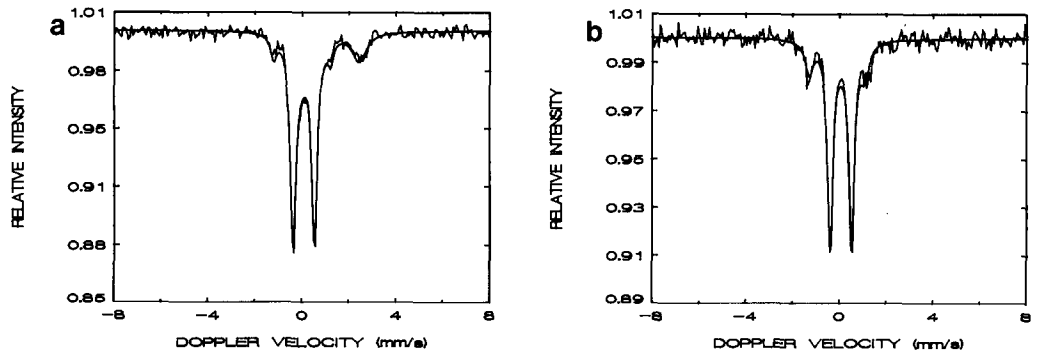

FIG. 2. Mössbauer spectra at 77 K after heating for 1 h at 323 K in H_2 flow. (a) $NEt_4[Fe_2Mn(CO)_{12}]$ catalyst and (b) $K[FeMn(CO)_9]$ catalyst.

TABLE 1

Mössbauer Parameters

Pretreatment	Figure	Sample	Species assigned	I.S.[a] (mm/s)	Q.S. (mm/s)	kOe	Relative area
Fresh sample	1a	$NEt_4[Fe_2Mn(CO)_{12}]$	$[Fe_2Mn(CO)_{12}]^-$	0.08	0.91		0.96
			D structure[c]	1.36	2.43		0.04
	1b	$K[HFe_3(CO)_{11}]$	$[HFe_3(CO)_{11}]^-$	0.04	1.38		0.64
				−0.01			0.36
	1c	$K[FeMn(CO)_9]$	$[Fe_2Mn(CO)_{12}]^-$	0.08	0.93		0.74
			$Fe(CO)_5$	−0.05	2.61		0.26
		$K[FeMn(CO)_9]$	$[Fe_2Mn(CO)_{12}]^-$	0.07	0.95		0.61
		Unsupported cluster	$Fe(CO)_5$	−0.07	2.67		0.39
323 K/1 h in H_2	2a	$NEt_4[Fe_2Mn(CO)_{12}]$	$[Fe_2Mn(CO)_{12}]^-$	0.08	0.91		0.68
			D structure[c]	1.21	2.42		0.25
			$Fe(CO)_5$	−0.01	2.42		0.07
	2b	$K[FeMn(CO)_9]$	$[Fe_2Mn(CO)_{12}]^-$	0.07	0.91		0.83
			$Fe(CO)_5$	−0.11	2.39		0.17
373 K/1 h in H_2	3a	$NEt_4[Fe_2Mn(CO)_{12}]$	$[Fe_2Mn(CO)_{12}]^-$	0.07	0.85		0.58
			D structure[c]	1.22	2.31		0.38
			$Fe(CO)_5$	−0.10	2.32		0.48
	3b	$K[HFe_3(CO)_{11}]$	$H[Fe_4(CO)_{13}]^-$	0.05	0.56		0.90
			$Fe(CO)_5$	−0.10	2.38		0.04
			D structure[c]	1.10	2.37		0.07
	3c	$K[FeMn(CO)_9]$	$H[Fe_4(CO)_{13}]^-$	0.01	0.53		0.92
			$Fe(CO)_5$	−0.10	2.52		0.06
			D structure[c]	1.23	2.47		0.04
423 K/1 h in H_2	4a	$NEt_4[Fe_2Mn(CO)_{12}]$	$H[Fe_4(CO)_{13}]^-$	0.08	0.61		0.84
			D structure[c]	1.12	2.45		0.16
	4b	$K[HFe_3(CO)_{11}]$	$H[Fe_4(CO)_{13}]^-$	0.08	0.61		0.79
			D structure[c]	1.18	2.32		0.21
473 K/2 h in H_2	5a	$NEt_4[Fe_2Mn(CO)_{12}]$	Fe^{3+}/carbide	0.43	0.86		0.43
			D structure[c]	1.21	2.13		0.57
	5b	$K[HFe_3(CO)_{11}]$	Fe^{3+}/carbide	0.37	0.68		0.58
			D structure[c]	1.10	2.26		0.41
	5c	$K[Fe_2Mn(CO)_{12}]$	Fe^{3+}/carbide	0.37	0.58		0.64
				1.10	2.27		0.36
	5d	$K[FeMn(CO)_9]$	Fe^{3+}/carbide	0.34	0.74		0.89
			D structure[c]	1.22	2.43		0.11
673 K/16 h in H_2	7a	$NEt_4[Fe_2Mn(CO)_{12}]$	D structure[c]	1.18	2.22		1.00
	7b	$K[Fe_2Mn(CO)_{12}]$	α-Fe	0.10[b]	−0.01	335.70	1.00
H_2/CO = 3, 2h	10a	$K[HFe_3(CO)_{11}]$	ε'-carbide			186.32	1.00
	10b	$NEt_4[Fe_2Mn(CO)_{12}]$	D structure[c]	1.29	2.08		1.00

[a] Isomer shift reported relative to that of a standard 1 mil iron foil (1 mil = 25.4 μm).

[b] Small positive isomer shifts for carbon-supported α-Fe particles are not unusual (*19, 33*).

[c] Isomer shift and quadrupole splitting refers only to the doublet component of the D-structure.

the same approximate amount in the $K[Fe_2Mn(CO)_{12}]$ sample at this stage. The second species produced both a singlet near 0 mm/s and a doublet with one peak at about 2.1 mm/s and the other near 0 mm/s, the latter of which has an isomer shift and

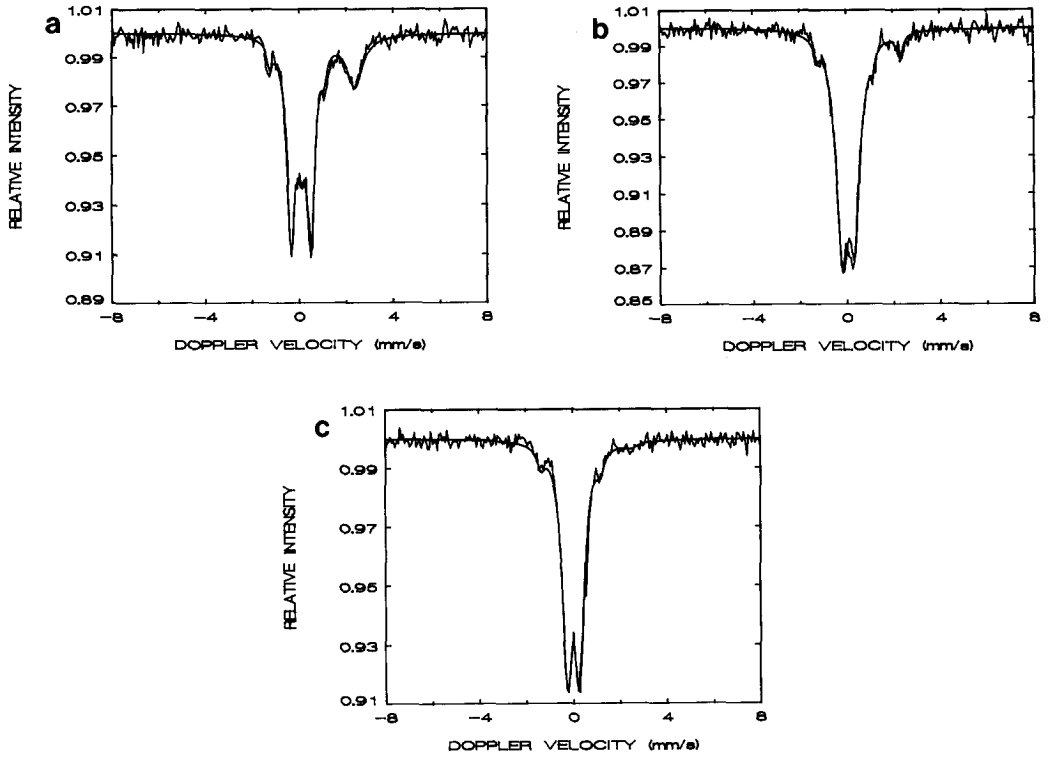

FIG. 3. Mössbauer spectra at 77 K after heating catalysts for 1 h at 373 K in H_2 flow: (a) $NEt_4[Fe_2Mn(CO)_{12}]$ catalyst, (b) $K[HFe_3(CO)_{11}]$ catalyst, and (c) $K[FeMn(CO)_9]$ catalyst.

quadrupole splitting characteristic of an oxide. The reported spectral areas include both doublet and singlet contributions, and the isomer and quadrupole splittings refer to the doublet portion. In an earlier study on carbon-supported $Fe_3(CO)_{12}$ clusters (*31*), it was pointed out that some uncertainty exists regarding the exact identification of this species; however, it has been postulated that it consists of a combination of superparamagnetic iron and Fe^{2+} ions interacting with oxygen. As in the previous study, it will be referred to as the "D-structure," since it is a product of the cluster decomposition process, and we believe it has a unique structure, as discussed later. After being heated to 323 K, the $K[HFe_3(CO)_{11}]$ catalyst gave a spectrum identical to the fresh sample (not shown to conserve space), and the $K[FeMn(CO)_9]$ sample showed a slight decrease in the amount of $Fe(CO)_5$ present compared to that of the fresh sample.

After being heated at 373 K, the spectra shown in Fig. 3 were obtained. In the case of the $NEt_4[Fe_2Mn(CO)_{12}]$ sample, the amounts of $Fe(CO)_5$ and the D-structure were increased, but in contrast, the $K[HFe_3(CO)_{11}]$, $K[FeMn(CO)_9]$, and $K[Fe_2Mn(CO)_{12}]$ clusters were converted to a new species consisting of a doublet with a decreased quadrupole splitting of about 0.6 mm/s. Some $Fe(CO)_5$ and the D-structure were also present in these last three samples, but in relatively small amounts compared to the new species. The identification of this species is discussed in more detail subsequently, but at this point is it worth noting that its MES parameters match those previously found for either of the anionic carbonyl clusters $[HFe_4(CO)_{13}]^-$ or $[HFe_2(CO)_8]^-$ (*28*). As shown in Figs. 4a

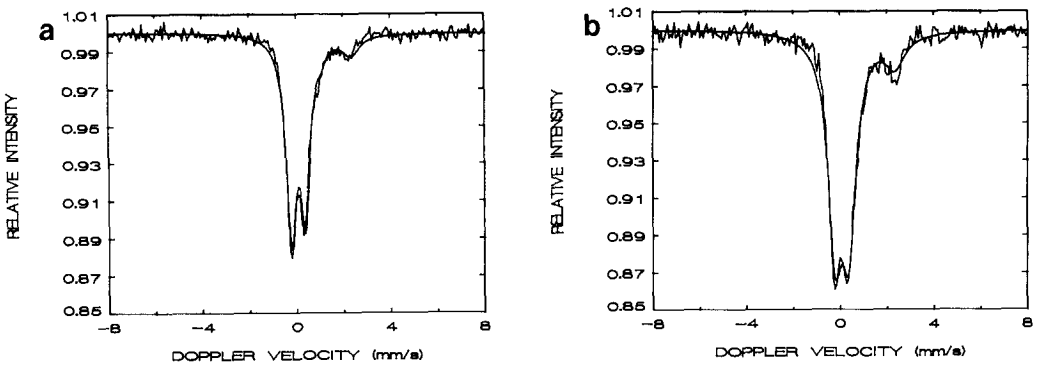

FIG. 4. Mössbauer spectra at 77 K after heating for 1 h at 423 K in H_2 flow: (a) $NEt_4[Fe_2Mn(CO)_{12}]$ catalyst and (b) $K[HFe_3(CO)_{11}]$ catalyst.

and 4b, no $Fe(CO)_5$ remained after heating for 1 h at 423 K, and in the case of the $NEt_4[Fe_2Mn(CO)_{12}]$ sample, the amount of the D-structure decreased. A similar decrease was found for the $K[FeMn(CO)_9]$ sample, which also showed a strong doublet attributable to the anionic clusters previously mentioned.

The spectra obtained after reducing the catalysts for 2 h at 473 K are shown in Fig. 5. For all the catalysts, the D-structure was present along with an additional peak just

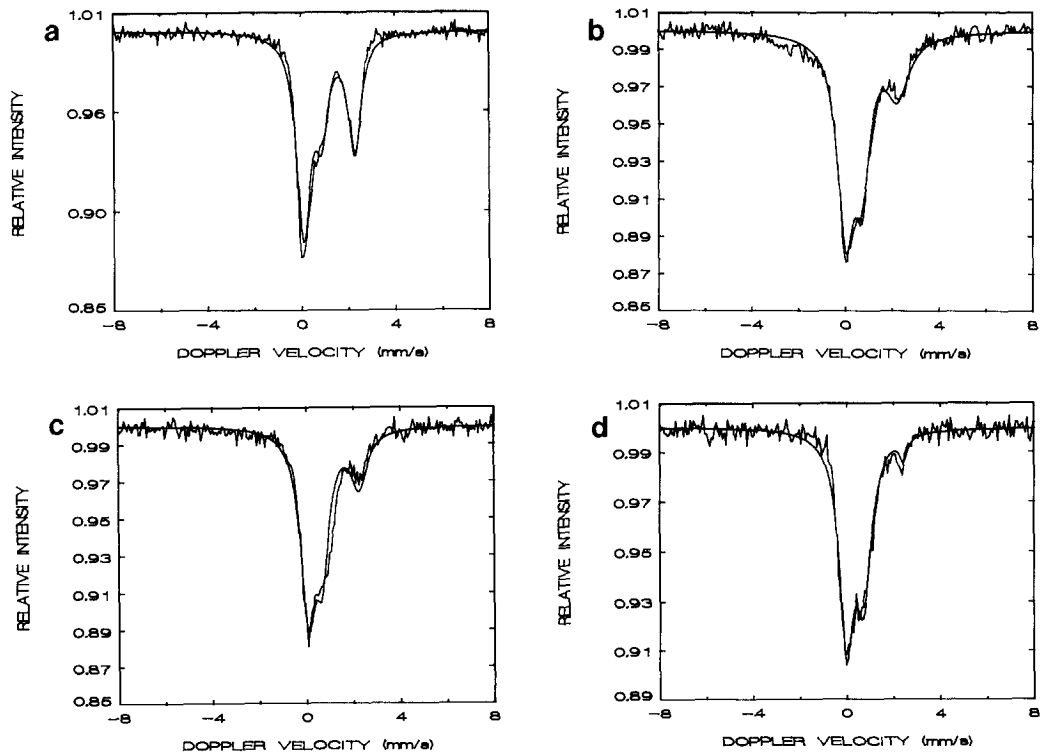

FIG. 5. Mössbauer spectra at 77 K after heating for 1 h at 473 K in H_2 flow: (a) $NEt_4[Fe_2Mn(CO)_{12}]$ catalyst, (b) $K[HFe_3(CO)_{11}]$ catalyst, (c) $K[Fe_2Mn(CO)_{12}]$ catalyst, and (d) $K[FeMn(CO)_9]$ catalyst.

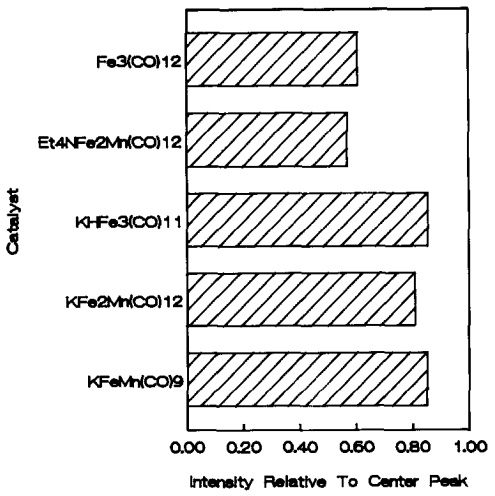

FIG. 6. Intensity of Mössbauer peak at 0.7 mm/s relative to the maximum absorption at 0 mm/s after pretreatment in H_2 for 2 h at 473 K. Data for $Fe_3(CO)_{12}$ sample are from Ref. (*31*).

to the right of the central peak. For fitting purposes, this additional peak was assumed to be the high velocity portion of a doublet whose other peak was at 0 mm/s. The intensity of this peak relative to the central peak increased sharply as a result of using K as a counter ion, as indicated in Fig. 6. This species is almost certainly an oxide or a carbide; however, as discussed later, it is difficult to distinguish between the two on the basis of the data collected here. In an attempt to identify this species, samples of the $NEt_4[Fe_2Mn(CO)_{12}]$ and $K[Fe_2Mn(CO)_{12}]$ catalysts were transferred to the LT cell and spectra were collected at 10 K. However, these spectra were very similar to those shown in Fig. 5, and no hyperfine splitting was observed.

Following the treatment at 473 K, CO was adsorbed on each catalyst at 298 K and 0.1 MPa. No changes in the spectra were detected as a result of the adsorption. The spectra were never magnetically split after the treatment at 473 K, indicating that the Fe dispersion in these catalysts remained quite high.

III. High Temperature Treatment in H_2

Following the decarbonylation and CO adsorption experiments, all the catalysts were treated at 673 K in flowing H_2 for 16 h. The resulting spectra for the $NEt_4[Fe_2Mn(CO)_{12}]$ and $K[Fe_2Mn(CO)_{12}]$ catalysts at 77 K are shown in Fig. 7. The $K[HFe_3(CO)_{11}]$ and $K[FeMn(CO)_9]$ spectra were similar in appearance to Fig. 7b; large α-Fe particles were detected, again with no indication of Mn being incorporated in the Fe particles. For the $K[HFe_3(CO)_{11}]$ sample the hyperfine field was slightly reduced from the value for bulk α-Fe (Table 1) indicating that the particles were "relaxed" and that the average particle size was probably below 15 nm (*32*). The isomer shift was slightly positive, which is not unusual for

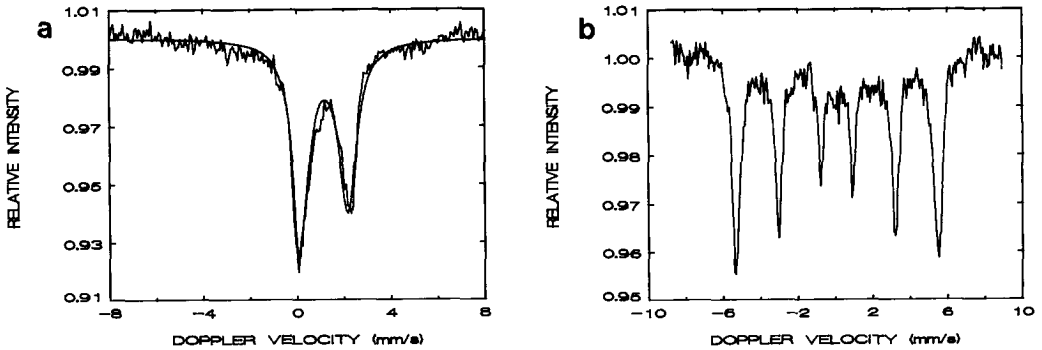

FIG. 7. Mössbauer spectra at 77 K of catalysts after reduction at 673 K for 16 h: (a) $NEt_4[Fe_2Mn(CO)_{12}]$ catalyst and (b) $K[Fe_2Mn(CO)_{12}]$ catalyst.

iron particles on carbon or graphite supports (*33*).

Consistent with the MES results, examination of the $K[Fe_2Mn(CO)_{12}]$ catalyst by electron microscopy showed the formation of groups of large metal particles (Fig. 8). While this group of large particles gave strong EDS signals for Fe and Mn, K was not detectable. This suggests that most of the K was contained in the areas of carbon vacated by the metal. However, because the olefin selectivity of this catalyst still remains much higher than that of an equivalently treated unpromoted catalyst (*21*), it is almost certain that some K remains on the surface of these metal particles.

Following the high temperature H_2 treatment, CO was again adsorbed on these samples at 298 K and 0.1 MPa. For all of the promoted catalysts, adsorption of CO had no effect on the spectrum, consistent with a large Fe particle size.

A completely different situation exists for the $NEt_4[Fe_2Mn(CO)_{12}]$ catalyst. This sample consisted largely of the D-structure, but the peak at 2.1 mm/s was slightly more intense than that in an Fe-only catalyst (*31*). For fitting purposes, only the D-structure was assumed to be present. CO adsorption at 298 K and 0.1 MPa produced peaks corresponding to $Fe(CO)_5$, indicating that at least a fraction of this phase was very well-dispersed. As in the case of the freshly impregnated catalyst, it was not possible to image any individual metal particles clearly in the STEM, even at high magnifications (Fig. 9). EDS measurements of the image area of Fig. 9 still show a Fe:Mn ratio of $Fe_2Mn_{1.26}$, close to the value expected from the precursor.

As a final step, all the samples were exposed to flowing syngas ($H_2/CO = 3$) at 498 K for 2 h. In the case of the $K[HFe_3(CO)_{11}]$, $K[Fe_2Mn(CO)_{12}]$, and $K[FeMn(CO)_9]$ samples, total carburization to ε'-carbide took place (Fig. 10a) based on the hyperfine splitting and isomer shift (*34*) found at 77 K. The fact that these catalysts carburized also implies an absence of Mn incorporation in the bulk of the Fe particles because previous studies of bulk Fe catalysts have shown that the presence of Mn inside bulk Fe suppresses carbide formation (*6, 12, 15*). The results here are consistent with previous MES studies which have shown that reduction of Fe and Fe–Mn catalysts at 523–673 K produced significant amounts of α-Fe that carburized under reaction conditions (*13, 35, 36*).

The spectrum of the $NEt_4[Fe_2Mn(CO)_{12}]$ sample did not change after a 2 h exposure to the H_2/CO mixture (Fig. 10b), nor was it altered by an additional 12-h exposure to the H_2/CO mixture. No hyperfine-split lines appeared from the sample in any state, implying that the particles were well-dispersed throughout the experiment. To investigate the D-structure of the $NEt_4[Fe_2Mn(CO)_{12}]$ catalyst further, a second sample from the same batch of C-supported $NEt_4[Fe_2Mn(CO)_{12}]$ was treated in exactly the same manner as the first sample. Following treatment at 673 K, the catalyst was transferred to the LT cell and peaks for α-Fe were obtained, but other components are also present. Most importantly, the outer line of a species with a hyperfine splitting greater than that of Fe is visible, as indicated by * in Fig. 11.

DISCUSSION

No MES studies have been reported for the precursor mixed-metal carbonyl clusters on a support surface; however, the excellent agreement of the MES parameters with the unsupported solid clusters shows that the clusters retain their integrity on carbon. This is also consistent with the DRIFTS spectra (*20*). On the basis of the MES evidence collected in this study, the initial carbonyl clusters are proposed to decompose via the formation of an Fe anionic intermediate, either $[HFe_4(CO)_{13}]^-$ or $[HFe_2(CO)_8]^-$. Although the MES parameters better fit the former species, clear evidence for the presence of the $[HFe_4(CO)_{13}]^-$ cluster only is provided by the DRIFTS spectra (*20*). As discussed in more detail

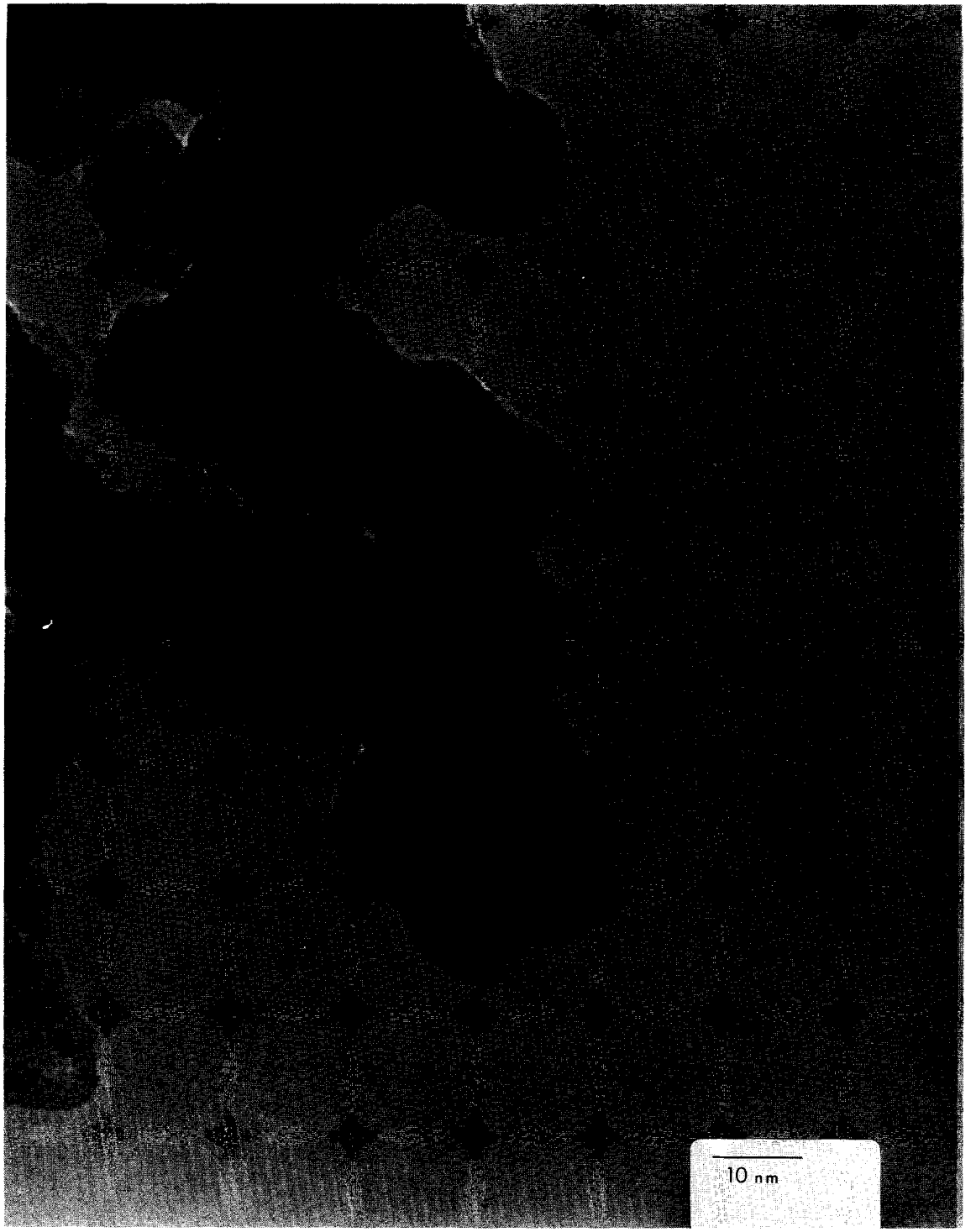

FIG. 8. Transmission electron micrograph of $K[Fe_2Mn(CO)_{12}]$ catalyst after 16 h reduction at 673 K. Strong EDS signals were obtained from the large particles; however, K was still not present in detectable amounts. Composition, $Fe_2Mn_{0.8}$.

FIG. 9. Transmission electron micrograph of $NEt_4[Fe_2Mn(CO)_{12}]$ catalyst after 16 h reduction at 673 K. Composition, $Fe_2Mn_{1.26}$.

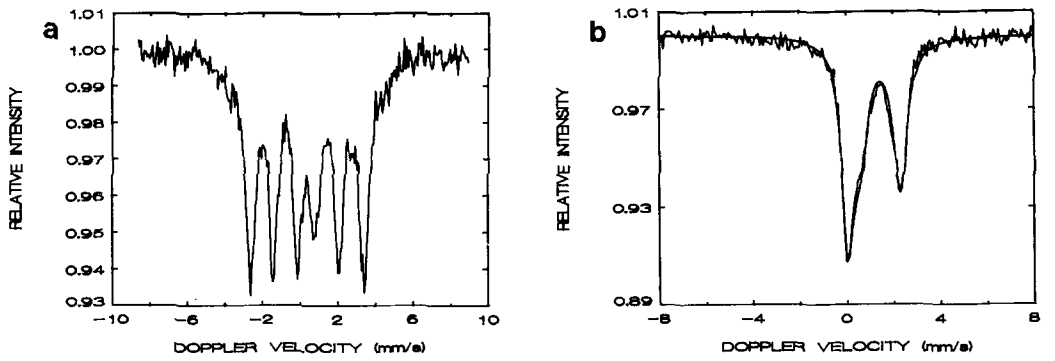

FIG. 10. Mössbauer spectra at 77 K after 2 h syngas flow (H_2/CO = 3) at 1 atm and 498 K. (a) $K[HFe_3(CO)_{11}]$ catalyst, $K[Fe_2Mn(CO)_{12}]$ and $K[FeMn(CO)_9]$ samples gave similar spectra after the same pretreatment. (b) $NEt_4[Fe_2Mn(CO)_{12}]$ catalyst. There was no change in the appearance of this spectrum after an additional 12 h of syngas flow at 498 K.

elsewhere, large amounts of $Mn_2(CO)_{10}$ were detected by DRIFTS during decarbonylation of the $K[Fe_2Mn(CO)_{12}]$ and $NEt_4[Fe_2Mn(CO)_{12}]$ clusters under H_2 (*20*). This observation is consistent with the formation of several possible Fe species, including $[HFe_4(CO)_{13}]^-$, $[HFe_2(CO)_8]^-$, $Fe_2(CO)_9$, $[HFe_3(CO)_{11}]^-$, or Fe in a positive oxidation state. The MES parameters obtained following decarbonylation at 323 K are not consistent with the presence of any of the last three compounds according to the previously published data on these species (*30, 37*). However, the dinuclear and tetranuclear anions are not reliably distinguished by MES since they have the same isomer shifts and their quadrupole splittings differ by less than 0.2 mm/s (*30*). The doubly negative $[Fe_4(CO)_{13}]^=$ anion can be ruled out because both the isomer shift and the quadrupole splittings are smaller than the values found in this study (*30*).

A previous X-ray study has shown that the $[HFe_4(CO)_{13}]^-$ cluster has a "butterfly" geometry in the crystalline state (*38*), with one of the CO ligands interacting with all four Fe atoms. The results obtained here agree in general with a recent MES study of the unsupported $[HFe_4(CO)_{13}]^-$ anion (*39*); however, the outer quadrupole doublet associated with one of the "wingtip" Fe atoms is not as pronounced in our spectra as in the unsupported cluster. One earlier report (*30*) has noted that the appearance of the outer doublet was variable, and it is presumed here that some distortion of the supported cluster may be responsible for the observed differences.

In all samples, $Fe(CO)_5$ was detected after decarbonylation at 323–373 K. The presence of this species is apparently governed by an interaction with the carbon support, because an identically prepared sample supported on graphite, which gives minimal surface interactions, shows no formation of $Fe(CO)_5$ (*40*). After being heated

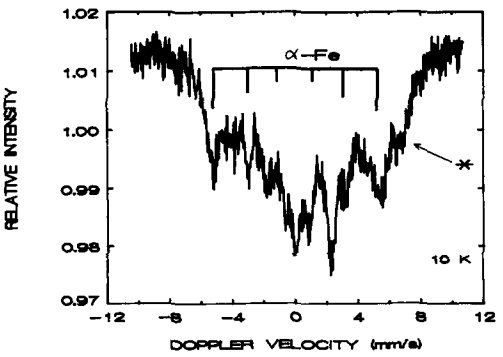

FIG. 11. Mössbauer spectrum at 10 K of the $NEt_4[Fe_2Mn(CO)_{12}]$ catalyst following reduction in H_2 at 673 K for 16 h. The sample was transferred to the low temperature cell in a N_2-purged glovebox prior to spectrum collection.

at 423 K, these $Fe(CO)_5$ clusters decomposed to yield additional highly dispersed superparamagnetic Fe.

The $[HFe_4(CO)_{13}]^-$ anion may be stabilized by a cationic species existing at the carbon surface; for example, the D-structure appearing in many of the spectra could be a source of stabilizing Fe ions. In an earlier study (*31*), this species was proposed to consist of two parts: superparamagnetically collapsed Fe or Fe carbide, plus Fe^{2+} ions coordinated to the carbon surface through oxygen atoms. This assignment is discussed more completely later. The interaction of $[Fe\text{-}C_5H_5]^{2+}$ cations with $[Fe_4(CO)_{13}]^{2-}$ anions has been reported in the literature (*41*), and it is postulated here that a similar interaction could occur between $[HFe_4(CO)_{13}]^-$ and Fe^{2+}, thereby forming larger clusters of Fe atoms. For the K-promoted catalysts, less of the D-structure was formed, and it is possible that some of the anions were stabilized with K^+ ions instead of Fe^{2+} ions.

During the final decarbonylation at 473 K all of the samples formed the D-structure plus an additional species which appeared as a peak immediately to the right of the central peak. Presumably, this side peak is a part of a doublet, whose other peak is near 0 mm/s. The assignment of this doublet is uncertain; however, at least three possibilities exist. First, the species could be an Fe–Mn mixed oxide; however, previous investigations (*42*) have shown that such oxides have a higher isomer shift than those observed in Fig. 5. Furthermore, a similar side peak also appeared in an earlier study of Fe-only catalysts (*31*), which argues against an Fe–Mn mixed-oxide species. Another possibility involves the formation of Fe carbide species via dissociation of CO from the carbonyl ligands on the Fe–Mn particle surface. As Cameron and Dwyer have shown recently (*43, 44*), CO can bond to Fe(100) surfaces through both the C and the O ends of the molecule in addition to adsorbing dissociatively. This allows the possibility for surface C to diffuse into the particles and form an Fe carbide species. A previous report of $Fe(CO)_5$ decomposition on graphite presents evidence favoring this alternative (*33*). In the present case, the carbide formed would have to be superparamagnetic, since no hyperfine-split peaks were obtained in the spectra after the 473 K pretreatment. The previously reported values of the isomer shift (0.23 mm/s) and quadrupole splitting (0.90 mm/s) for superparamagnetic ε'-carbide were obtained at room temperature (*34, 45*). The isomer shifts reported here are clearly larger than those reported earlier; however, in theory and in practice (*25*), isomer shifts become progressively more positive as the temperature is lowered. Thus, the values measured here are consistent with those expected for iron carbide. A final alternative is that this doublet represents an Fe^{3+} oxide species. This possibility is supported by a previous investigation where carbon-supported, Fe-only catalysts were reduced at 473 K and then deliberately oxidized in air (*31*). Upon rereduction in flowing H_2 at 473 K, a spectrum similar to that in Fig. 7a was obtained. No oxygen contribution is expected from the carbon surface because it was handled in an inert atmosphere subsequent to a high temperature H_2 treatment, which removes oxygen groups from the surface (*46, 47*). However, the oxygen could be provided by the dissociation of CO produced during the decarbonylation process. While it is not possible to distinguish between the last two alternatives (i.e., carbide vs oxide) based on the evidence here, the fact that the side peak increases in intensity when K is added implies that its formation is facilitated by CO dissociation, because previous results have shown that K enhances CO dissociation on Fe surfaces (*44, 48*).

After the H_2 pretreatment at 473 K, no MES evidence was found to indicate the presence of bulk Fe_2MnO_4 in the bimetallic catalysts. Nevertheless, for the $NEt_4[Fe_2Mn(CO)_{12}]$ cluster in particular, past studies have shown that enhanced olefin se-

lectivity exists after pretreatment at 473 K (*18*). These observations taken together imply that the spinel phase, if it exists at all, is confined to the surface of the Fe–Mn particles. It is possible that, because of the small particle sizes involved, the spinel phase is superparamagnetic, but a previous study has shown that Fe_2MnO_4 particles as small as 6–19 nm still show hyperfine splitting (*49*), although the value is reduced from the bulk value reported elsewhere (*50, 51*). Apparently no studies have been performed on Fe_2MnO_4 particles so small that the hyperfine field completely collapses, so the existence of extremely small spinel particles or a surface spinel structure cannot be ruled out. On the basis of the observation that $Mn_2(CO)_{10}$ formed as the cluster decomposed, a more likely scheme is that the Mn exists as small Mn oxide (most likely MnO) particles dispersed on the surface of the D-structure Fe particles.

Metal Structure following High Temperature Treatment in H_2

In all the catalysts made from clusters containing potassium, the iron and manganese phases separated during high temperature reduction and the iron formed large α-Fe particles, which is in agreement with previous work on the reduction behavior of Fe–Mn oxides and spinel structures (*3, 11, 12, 52*). This is clearly seen in the unrelaxed MES spectrum (Fig. 7b), and TEM shows that the resulting metal particles on carbon are very large, i.e., 20–30 nm (Fig. 8), yet no intermetallic compounds were detected in any of these catalysts by MES. Regardless, the CO uptakes at 195 K on these samples are significantly higher than expected for iron crystallites of this size (*21*). It is possible that during phase segregation small iron zones form along with MnO zones, and the large particles observed by TEM are composed of a mixture of these smaller zero-valent Fe and MnO zones. Oxidation of large Fe–Mn particles followed by a HTR step produced such small segregated zones of iron (*54*). The MES spectra of large particles consisting of an agglomerate of such a mixture of smaller iron and MnO zones would probably be identical to that of a single large iron crystallite because of the strong interaction anisotropy (*55*) between the iron zones, yet the iron surface area would be much higher than that of a single large iron crystallite. In contrast, particles produced from the cluster containing no potassium, i.e., $NEt_4[Fe_2Mn(CO)_{12}]$, remained well dispersed after reduction at 673 K. In fact, the MES spectrum (Fig. 7a) was unchanged (the D-structure). Also, no particles were visible in the TEM micrographs. Further characterization of this catalyst indicated that a small amount of $Fe(CO)_5$ reformed during CO adsorption at 300 K following high temperature reduction, and the olefin selectivity dropped in the CO/H_2 reaction (*18, 21*). These observations are consistent with a catalyst initially consisting, at least partially, of small, zero-valent Fe particles.

The fact that particles made from K-containing clusters sinter readily is not surprising. Potassium is known, empirically, to promote sintering of bulk iron catalysts (*53*), and its role in facilitating agglomeration of Fe on carbon-supported catalysts has been observed before (*18*). One possible explanation is that the potassium blocks the active sites on the carbon surface, effectively removing all stabilizing "anchor" sites and allowing the metal to sinter rapidly as it does on graphite supports (*54*). This is discussed in greater detail in the third paper in this series (*21*).

It is most likely that the D-structure consists of a combination of superparamagnetic, zero-valent iron and an Fe^{2+} oxide species (*31*). Similar peak positions and relative intensities have been reproducibly obtained in a number of iron/carbon systems (*31, 35, 40*) and, in addition, this spectrum has never been reported for iron dispersed on refractory oxide supports. Therefore, it seems probable that the Fe^0 and Fe^{2+} species are present in a well-defined configuration, rather than an arbitrary

mixture of two phases, hence our designation as the D (for decomposition)-structure. The MES spectrum at 10 K provides additional information regarding the morphology of the D-structure. Indeed, it can readily be seen in Fig. 11 that a significant amount of α-iron is present. This is consistent with the work of others on Fe-only particles on carbon. Niemantsverdriet *et al.* reported spectra of Fe in the D-structure at 300 and 77 K, and they found that these spectra resolved primarily into α-Fe at 4 K (*36*).

The low temperature spectra also suggest there is interaction between the iron and the manganese. The presence of a peak on the far right and the absence of companion peak on the far left suggest the presence of a species with a large hyperfine field and a large positive isomer shift. This is regarded as circumstantial evidence that an oxide phase is also present. In contrast, it was found in both the present study (*40*) and an earlier study (*36*) that for iron-only structures on carbon, which have spectra nearly identical to those reported here at 300 and 77 K, no such peak exists in the low temperature spectrum. This suggests that manganese and iron do interact to some extent, possibly forming a mixed-metal oxide.

A question remains about the state of the Fe–Mn catalyst under flowing syngas at 498 K. The MES data clearly show that the iron in the particles produced from potassium-containing clusters forms ε-carbide (Fig. 10a). This is not surprising as it was previously shown that the iron and manganese were phase separated in these particles during high temperature reduction, and it is generally expected that iron will carburize during CO hydrogenation over its surface (*25, 34, 45*). However, the state of the iron in the $NEt_4[Fe_2Mn(CO)_{12}]$ catalysts is not as clear. Although the Mössbauer spectra suggest that little change took place under synthesis gas at 498 K (Fig. 10b), it is possible that the metallic component of the D-structure was fully carburized. Superparamagnetic carbide and superparamagnetic α-iron are difficult to distinguish, as shown in the earlier study by Niemantsverdriet *et al.* (*36*).

ACKNOWLEDGMENTS

This study was supported by the National Science Foundation under grant CBT-8619619. Partial support of A.A.C. by a Texaco Philanthropic Foundation Fellowship is gratefully noted. The authors thank Dr. George Wagner, Mr. John Johnson, and Professor G. L. Geoffroy for their help in synthesizing the carbonyl cluster precursors used in this study.

REFERENCES

1. Soled, S. L., and Fiato, R. A., U.S. Patent 4,604,375 (1986).
2. Fiato, R. A., and Soled, S. L., U.S. Patent 4,621,102 (1986).
3. Jensen, K. B., and Massoth, F. E., *J. Catal.* **92,** 98 (1985).
4. Jensen, K. B., and Massoth, F. E., *J. Catal.* **92,** 109 (1985).
5. Zhuravleva, M. G., Chufarov, G. I., and Brainina, D. Z., *Dokl. Acad. Nauk SSSR* **132,** 1074 (1960).
6. Lochner, U., Papp, H., and Baerns, M., *Appl. Catal.* **23,** 339 (1986).
7. Barrault, J., Renard, C., Yu, L. T., and Gal, J., *in* "Proceedings, 8th International Congress on Catalysis, Berlin, 1984," Vol. 2, p. 101. Dechema, Frankfurt-am-Main, 1984.
8. Gryzbek, T., Papp, H., and Baerns, M., *Appl. Catal.* **29,** 335 (1987).
9. Stencel, J. M., Diehl, J. R., Miller, S. R., Anderson, R. A., Zarochak, M. F., and Pennline, H. W., *Appl. Catal.* **33,** 129 (1987).
10. Barrault, J., and Renard, C., *Appl. Catal.* **14,** 133 (1985).
11. Jaggi, N. K., Schwartz, L. H., Butt, J. B., Papp, H., and Baerns, M., *Appl. Catal.* **13,** 347 (1985).
12. Maiti, G. C., Malessa, R., and Baerns, M., *Appl. Catal.* **5,** 151 (1983).
13. Maiti, G. C., Malessa, R., Lochner, U., Papp, H., and Baerns, M., *Appl. Catal.* **16,** 215 (1985).
14. Deppe, P., Papp, H., and Rosenberg, M., *Hyperfine Interact.* **28,** 903 (1986).
15. Lohrengel, G., and Baerns, M., *Ber. Bunsen. Ges. Phys. Chem.* **87,** 335 (1983).
16. Bruce, L., Hope, G., and Turney, T. W., *React. Kinet. Catal. Lett.* **20,** 175 (1982).
17. Kuznetsov, V. L., Danilyuk, H. F., Kolosova, I. E., and Yermakov, Y. I., *React. Kinet. Catal. Lett.* **21,** 249 (1982).
18. Venter, J., Kaminsky, M., Geoffroy, G. L., and Vannice, M. A., *J. Catal.* **103,** 450 (1987); **105,** 155 (1987).

19. Phillips, J., and Dumesic, J. A., *Appl. Catal.* **9,** 1 (1984).
20. Venter, J. J., Chen, A. A., and Vannice, M. A., *J. Catal.* **117,** 170 (1989).
21. Venter, J. J., Chen, A. A., Phillips, J., and Vannice, M. A., *J. Catal.*, in press.
22. Ruff, J. K., *Inorg. Chem.* **7,** 1818 (1968).
23. Hodali, H. A., Arcus, C., and Shriver, D. F., *Inorg. Synth.* **20,** 218 (1980).
24. Shriver, D. F., and Drezdzon, M. A., "The Manipulation of Air-Sensitive Compounds," 2nd ed. Wiley-Interscience, New York, 1986.
25. Lin, S. C., and Phillips, J., *J. Appl. Phys.* **58,** 1943 (1985).
26. Sorenson, K., Internal Report No. 1, Laboratory of Applied Physics, Technical University of Denmark, Lyngby, Denmark, 1972.
27. Wood, J. E., Williams, D. B., and Goldstein, J. I., *J. Microsc.* **133,** 255 (1984).
28. Cooke, C. G., and Mays, M. J., *J. Organomet. Chem.* **74,** 449 (1974).
29. Lindauer, M. W., Spiess, H. W., and Sheline, R. K., *Inorg. Chem.* **9,** 1694 (1970).
30. Farmery, K., Kilner, M., Greatrex, R., and Greenwood, N. N., *J. Chem. Soc. A,* 2339 (1969).
31. Chen, A. A., Vannice, M. A., and Phillips, J., *J. Phys. Chem.* **91,** 6257 (1987).
32. Morup, S., Dumesic, J. A., and Topsoe, H., *in* "Applications of Mössbauer Spectroscopy" (R. L. Cohen, Ed.), Vol. 2, p. 1. Academic Press, New York, 1980.
33. Phillips, J., Clausen, B., and Dumesic, J. A., *J. Phys. Chem.* **84,** 1814 (1980).
34. Amelse, J. A., Butt, J. B., and Schwartz, L. H., *J. Phys. Chem.* **82,** 558 (1978).
35. Van Dijk, W. L., Niemantsverdriet, J. W., Van der Kraan, A. M., and Van der Baan, H. S., *Appl. Catal.* **2,** 273 (1982).
36. Niemantsverdriet, J. W., Van der Kraan, A. M., Delgass, W. N., and Vannice, M. A., *J. Phys. Chem.* **89,** 67 (1985).
37. Greenwood, N. N., and Gibb, T. C., "Mössbauer Spectroscopy." Chapman and Hall, London, 1971.
38. Manassero, M., Sansoni, M., and Longoni, G., *J. Chem. Soc. Chem. Commun.*, 919 (1976).
39. Benson, G. G., Long, G. J., Bradley, J. S., Kolis, J. W., and Shriver, D. F., *J. Amer. Chem. Soc.* **108,** 1898 (1986).
40. Chen, A. A., Ph.D. thesis, The Pennsylvania State University, 1988.
41. Doedens, R. J., and Dahl, L. F., *J. Amer. Chem. Soc.* **88,** 4847 (1966).
42. Hope, D. A. O., Cheetham, A. K., and Long, G. J., *Inorg. Chem.* **21,** 2804 (1982).
43. Cameron, S. D., and Dwyer, D. J., *Langmuir* **4,** 282 (1988).
44. Cameron, S. D., and Dwyer, D. J., *Surf. Sci.* **198,** 315 (1988).
45. Raupp, G. B., and Delgass, W. N., *J. Catal.* **58,** 348, 361 (1979).
46. Puri, R. B., Kumar, B., and Sing, D. D., *J. Sci. Res. (India)* **200,** 366 (1961).
47. Smith, R. N., Duffield, J., Pierotti, R. A., and Mooi, J., *J. Phys. Chem.* **60,** 495 (1956).
48. Broden, G., Gafner, G., and Bonzel, H. P., *Surf. Sci.* **84,** 295 (1979).
49. Vandenberghe, R. E., Vanleerberghe, R., and Gryffroy, D., *Phys. Lett.* **101A,** 297 (1984).
50. Armstrong, R. J., Morrish, A. H., and Sawatzky, G. A., *Phys. Lett.* **23,** 414 (1966).
51. Sawatzky, G. A., Van Der Woude, F., and Morrish, A. H., *Phys. Lett.* **25A,** 147 (1967).
52. Colombo, U., Gazzarini, F., and Lanzavecchia, G., *Mater. Sci. Eng.* **2,** 125 (1967).
53. Dry, M. E., and Oosthuizen, G. J., *J. Catal.* **11,** 18 (1968).
54. Chen, A. A., Vannice, M. A., and Phillips, J., *J. Catal.* **115,** 568 (1989).